0022-3565/02/3023-1158–1167$7.00
THE JOURNAL OF PHARMACOLOGY AND EXPERIMENTAL THERAPEUTICS
Vol. 302, No. 3
4875/1005382
Printed in U.S.A.

JPET 302:1158–1167, 2002

Mechanism-Based Pharmacokinetic-Pharmacodynamic Modeling of Concentration-Dependent Hysteresis and Biphasic Electroencephalogram Effects of Alphaxalone in Rats

S. A. G. VISSER, C. J. G. M. SMULDERS, B. P. R. REIJERS, P. H. VAN DER GRAAF, L. A. PELETIER, and M. DANHOF

Division of Pharmacology, Leiden/Amsterdam Center for Drug Research, Leiden University, Leiden, The Netherlands (S.A.G.V., C.J.G.M.S., B.P.R.R., M.D.); Pfizer Global Research & Development, Discovery Biology, Sandwich, Kent, United Kingdom (P.H.v.d.G.); Mathematical Institute, Leiden University, Leiden, The Netherlands (L.A.P.)

Received December 26, 2001; accepted May 10, 2002 This article is available online at http://jpet.aspetjournals.org

ABSTRACT

The neuroactive steroid alphaxalone reveals a complex biphasic concentration-effect relationship using the 11.5 to 30 Hz frequency band of the electroencephalogram (EEG) as biomarker. The purpose of the present investigation was to develop a mechanism-based pharmacokinetic-pharmacodynamic model to describe this observation. The proposed model is based on receptor theory and aims to separate the drug-receptor interaction from the transduction of the initial stimulus into the observed biphasic response. Individual concentration-time courses of alphaxalone were obtained in combination with continuous recording of the EEG parameter. Alphaxalone was administered intravenously in various dosages. The pharmacokinetics were described by a two-compartment model, and parameter estimates for clearance, intercompartmental clearance, volume of distribution 1 and 2 were 158 ± 29 ml · min^{-1} · kg^{-1}, 143 ± 31 ml · min^{-1} · kg^{-1}, 122 ± 20 ml · kg^{-1} and 606 ± 48 ml · kg^{-1}, respectively. Concentration-effect relationships exhibited a biphasic pattern and delay in onset of effect. The hysteresis was described on the basis of an effect-compartment model with C_{max} as covariate. The pharmacodynamic model consisted of a receptor model, featuring a monophasic saturable receptor activation model in combination with a biphasic stimulus-response model. The in vivo affinity (K_{PD}) was estimated at 432 ± 26 ng · ml^{-1}. Unique parameter estimates were obtained that were independent of the dose and the duration of the infusion. In conclusion, we have shown that this mechanism-based approach, which separates drug- and system-related properties in vivo, was successfully applied for the characterization of the biphasic effect versus time patterns of alphaxalone. The model should be of use in the characterization of other biphasic responses.

The sedative-hypnotic and anesthetic properties of a wide range of natural and synthetic steroids were first shown by Selye (1942). This initial work led to the introduction of the synthetic neuroactive steroid alphaxalone (5α-pregnan-3α-ol-11,20-dione) into clinical medicine (Sear, 1996). Alphaxalone exerts its selective action via a specific binding site at the $GABA_A$ receptor complex and does not interact with any of the classical cytosolic hormonal steroid receptors (Paul and Purdy, 1992; Lambert et al., 1995). Detailed mechanistic investigations have revealed a dual mechanism of action for alphaxalone. Low concentrations of alphaxalone allosterically modulate the amplitude of GABA-induced ion currents, whereas alphaxalone at higher concentrations (≥1 μM) acts as an agonist, similar to that observed by barbiturates (Cottrell et al., 1987; Paul and Purdy, 1992; Lambert et al., 1995). Recently, there has been a renewed interest in neuroactive steroids in relation to the development of novel strategies for the treatment of anxiety, insomnia, migraine, depression, and seizure disorders (Gasior et al., 1999). However, very few attempts have been made to study neuroactive steroids in vivo on the basis of an integrated PK/PD approach.

In recent years, considerable progress has been made in the elucidation of the PK/PD models of drugs acting at

Preliminary results were presented at the British Pharmacological Society meeting January 2000 [Visser SAG, Smulders CJGM, Van der Graaf PH, and Danhof M (2000) Biphasic and dose-dependent in vivo time course of $GABA_A$-receptor-mediated EEG effects of the neurosteroid alphaxalone, in rats. *Br J Pharmacol* **129:**81].

ABBREVIATIONS: PK/PD, pharmacokinetic-pharmacodynamic; EEG, electroencephalogram; HPLC, high pressure liquid chromatography; CL, total body clearance; Q, intercompartmental clearance; V_1 and V_2, volumes of distribution of compartment 1 and 2; V_{dss}, volume of distribution at steady state; C_{max}, maximal concentration reached in plasma; DMSO, dimethylsulfoxide; HPβCD, 2-hydroxypropyl-β-cyclodextrin; f_u, fraction unbound; k_{eo}, equilibration rate constant for hysteresis; E_0, baseline EEG; E_{top}, maximal EEG effect; e_{PD}, in vivo drug efficacy; K_{PD}, in vivo drug affinity; *a*, coefficient determining steepness of the parabola; *b*, stimulus intensity where the top of the parabola is reached; *d*, exponent determining the asymmetry of the parabola.

$GABA_A$ receptors (i.e., allosteric modulators such as benzodiazepines and the GABA re-uptake inhibitor tiagabine) using quantitative EEG parameters as pharmacodynamic endpoint (Danhof and Mandema, 1992; Cleton et al., 1999a) . In a preliminary in vivo PK/PD study, alphaxalone was shown to exhibit biphasic EEG effects (Visser et al., 1990). The time-EEG effect profiles showed an increase in effect at low drug concentrations and a decrease in effect at higher drug concentrations. Similar biphasic patterns have been observed for general anesthetics, such as propofol, heptabarbital, amobarbital, and thiopental (Mandema and Danhof, 1990; Ebling et al., 1991; Mandema et al., 1991; Cox et al., 1998b).

Several methods have been proposed to characterize biphasic drug concentration-effect relationships. The most frequently used method is a nonparametric analysis of the concentration-effect data (Ebling et al., 1991). In this method, descriptive pharmacodynamic parameters are obtained on the basis of linear interpolation between the data points. A limitation of this approach is that it is entirely descriptive, with no predictive or explanatory value. Another method to characterize biphasic PK/PD relationships is a biphasic model constructed from various combinations and modifications of the nonlinear sigmoid E_{max} model, which was first proposed by Paalzow and Edlund (1979) and applied by Mandema and Danhof (1990). This model was based on the observation that biphasic effects were mediated by multiple (two) receptor responses. Although this dual effect model is conceptually simple and relatively easy to parameterize, good parameter estimates can only be obtained if the ratio between the IC_{50} and the EC_{50} is at least 300 (Dutta and Ebling, 1997). Furthermore, the mechanistic basis of such a model is not always clear.

In recent years, an important development in PK/PD analysis has been the design of an entirely new class of mechanism-based PK/PD models (Van der Graaf and Danhof, 1997). A specific feature of these models is that a clear separation is made between a drug-specific part, characterizing the drug receptor interaction in terms of in vivo affinity and intrinsic efficacy, and a system-specific part, characterizing the in vivo stimulus-response relationship (Cox et al., 1998a; Tuk et al., 1999; Van der Graaf et al., 1999; Zuideveld et al., 2001). To date, in this approach both linear and nonlinear (hyperbolic) stimulus-response relationships have been considered. In theory, however, a stimulus-response relationship can take any shape and it can also be biphasic.

In this investigation, we propose a mechanism-based PK/PD model in which the initial receptor activation is monophasic and saturable, whereas the subsequent transduction is biphasic. In the model, the receptor activation is described by a hyperbolic function and the biphasic transduction part by a parabolic function (see Fig. 1). To validate the model, we have obtained high resolution concentration and effect data for the synthetic neuroactive steroid alphaxalone in several dosages and infusion rates.

Materials and Methods

Animals and Surgical Procedures. Male Wistar rats (301 ± 7 g, n = 44; Charles River BV, Zeist, The Netherlands) were used in this investigation. Following surgery, the rats were housed individually in standard plastic cages with a normal 12-h day/night schedule (lights on 7 AM) at a temperature of 21°C. The animals had

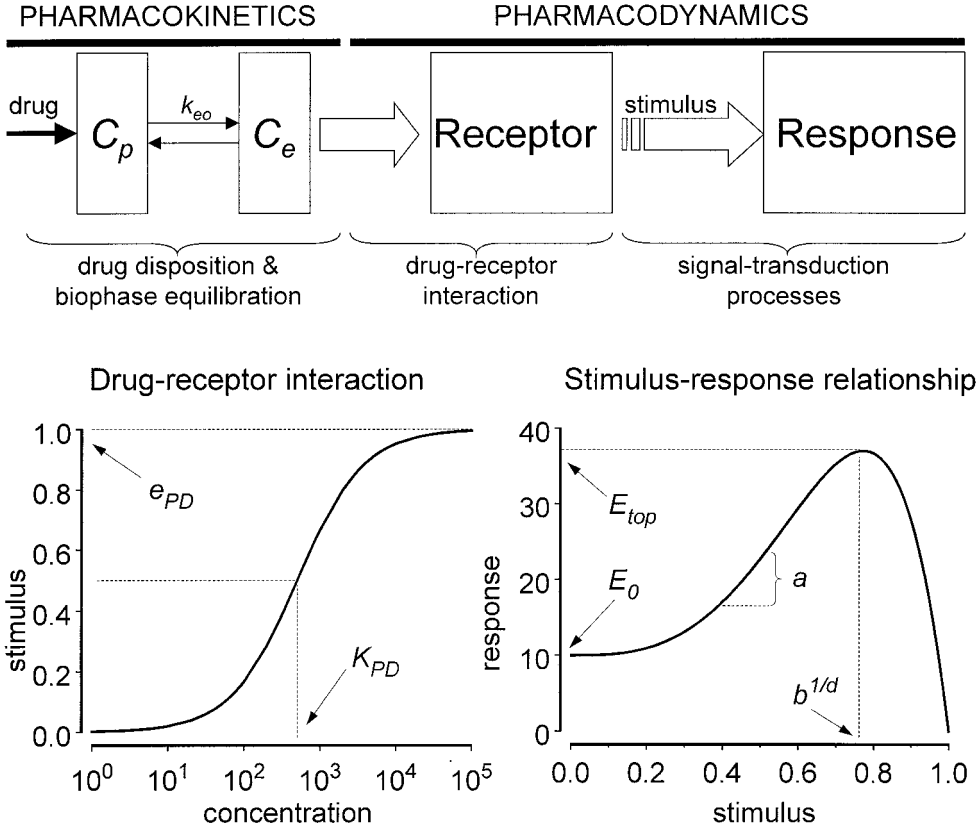

Fig. 1. Schematic view of the mechanism-based PK/PD approach. The pharmacokinetics describe the disposition of the drug in the plasma (C_p) and equilibration to the biophase (effect-site, C_e), where the drug can activate the receptor. Upon activation of the receptor, a stimulus is produced which leads to the response via several signal-transduction processes (pharmacodynamics). The proposed model consists of two parts. The first part consists of a model for drug receptor interaction (eq. 15), which is a hyperbolic function of the effect-site concentration producing a stimulus. K_{PD} is the concentration producing the half-maximal stimulus and e_{PD} is the maximal stimulus. The second part consists of a biphasic stimulus-response model, which is represented by a parabolic function (eq. 19). E_0 is baseline response, the top of the stimulus-response relationship is located at the value E_{top} and is obtained at the value $b^{1/d}$ and the slope of the parabolic function is determined by a.

access to standard laboratory chow (RMH-TM; Hope Farms, Woerden, The Netherlands) and acidified water ad libitum.

Nine days before the start of the experiments seven cortical electrodes were implanted into the skull as described before (Mandema and Danhof, 1990). Briefly, the electrodes were placed at the locations 11 mm anterior and 2.5 mm lateral (F_l and F_r), 3 mm anterior and 3.5 mm lateral (C_l and C_r), and 3 mm posterior and 2.5 mm lateral (O_l and O_r) to lambda. A reference electrode was placed on lambda. Stainless steel screws were used as electrodes and connected to a miniature connector, which was insulated and fixed to the skull with dental acrylic cement. The surgical procedures were performed under anesthesia with 0.1 mg · kg^{-1} i.m. of medetomidine hydrochloride (Domitor; Pfizer, Capelle a/d IJssel, The Netherlands) and 1 mg · kg^{-1} s.c. of ketamine base (Ketalar; Parke-Davis, Hoofddorp, The Netherlands). After the first surgery, 4 mg of ampicillin (A.U.V., Cuijk, The Netherlands) was administered to aid recovery.

Three days before the start of the experiment, indwelling cannulae were implanted in the right femoral artery for the serial collection of arterial blood samples and in the right jugular vein for drug administration. The cannulae were filled with heparinized 25% (g/v) polyvinylpyrrolidone in saline (Brocacef, Maarssen, The Netherlands) and tunneled subcutaneously to the back of the neck where they were exteriorized and fixed with a rubber ring. The protocol of this investigation was approved by the Ethical Committee on Animal Experimentation of Leiden University.

Drugs and Dosages. Alphaxalone (5α-pregnan-3α-ol-11,20-dione) was purchased from Sigma-Aldrich BV (Zwijndrecht, The Netherlands). Rats were randomly assigned to six treatment groups of 6 to 8 rats that each received a zero-order intravenous infusion of alphaxalone over 5 or 15 min. A summary of the various infusion regimens is given in Table 1. Two different vehicles were used to formulate alphaxalone: 1) 100 μl of dimethyl sulfoxide (DMSO; Baker, Deventer, The Netherlands); and 2) 100 μl of 25% (w/v) 2-hydroxypropyl-β-cyclodextrin (HPβCD; Sigma-Aldrich BV). Vehicle controls were included in all treatment groups.

Pharmacokinetic-Pharmacodynamic Experiments. All experiments were started between 830 and 930 AM to exclude influences of circadian rhythms. The rats were placed in a rotating drum to control the level of vigilance, thereby avoiding the interference of sleep patterns. During the experiments, the rat was deprived of food and water. Two bipolar EEG leads (C_l-O_l) and (C_r-O_r) were continuously recorded using a Nihon-Kohden AB-621G Bioelectric amplifier (Hoekloos BV, Amsterdam, The Netherlands) and concurrently digitized at a rate of 256 Hz using a CED 1401_{plus} interface (Cambridge Electronic Design Ltd., Cambridge, UK). The digitized signal was fed into a Pentium III computer and stored on a hard disk for off-line analysis. After recording the EEG baseline for 45 min, a zero-order intravenous infusion of alphaxalone was administered to the conscious and freely moving rats using an infusion pump (BAS Bioanalytical Systems Inc., West Lafayette, IN). The EEG recordings lasted until 120 min after the end of the infusion. For each 5-s epoch, quantitative EEG parameters were obtained off-line by fast Fourier transformation with a user-defined program within the data analysis software package Spike 2 for Windows, version 3.18 (Cambridge Electronic Design Ltd.). Amplitudes in the β-frequency band of the EEG (11.5–30 Hz) averaged over 25-s time intervals were used to quantify the drug effect. Serial arterial blood samples were collected at predefined time intervals in heparinized tubes and centrifuged at 5000 rpm for 15 min for plasma collection. Total volume of redrawn blood samples was kept equal to 2.1 ml during each experiment. Drug samples were stored at −20°C until HPLC analysis.

HPLC Analysis. Alphaxalone plasma concentrations were determined using HPLC as described before (Visser et al., 2000). Briefly, to 50 μl of plasma, 50 μl of the internal standard (1.5 $\mu g \cdot ml^{-1}$ pregnenolone dissolved in acetonitrile) was added. Subsequently, 200 μl of acetonitrile was added to precipitate plasma proteins. After centrifugation, the supernatant was transferred to a clean tube and 50 μl of 2 M NaOH and 25 μl of dansylhydrazine solution (20 mg in methanol acidified with 40 μl of sulfuric acid) were added. After incubation at room temperature for 20 h at a dark place, 500 μl of 1 M NaOH and 5 ml of dichloromethane were added, and the mixture was vortexed for 5 min. The phase system was centrifuged for 15 min at 4500*g*, and the organic phase was transferred to a clean tube and evaporated under reduced pressure on a vortex vacuum evaporator (Labconco Corp., Kansas City, MO) at 37°C. The residue was dissolved in 100 μl of mobile phase, of which a volume of 50 μl was injected into the HPLC system.

The HPLC system consisted of a Waters 501 solvent delivery pump, a Waters 717plus autosampler (Millipore-Waters, Milford, MA) and a Jasco FP 1520 intelligent fluorescence detector (Jasco Co., Tokyo, Japan). Chromatography was performed on a C_{18} 3-μm cartridge column (100 × 4.6 mm i.d.; Chrompack, Bergen op Zoom, The Netherlands) equipped with a guard column. The mobile phase consisted of a mixture of 25 mM acetate buffer (pH 3.7) and acetonitrile (45:55 v/v). Flow rate was 1 ml · min^{-1}. Fluorescence detection occurred at excitation wavelength 332 nm and emission wavelength 516 nm. Data acquisition and processing was performed using a Chromatopac C-R3A reporting integrator (Shimadzu, Kyoto, Japan). Linear calibration curves were obtained in the range 0.01 to 10 $\mu g \cdot ml^{-1}$ ($r > 0.990$, $n = 17$), and the limit of quantification was 0.01 $\mu g \cdot ml^{-1}$. The intra-assay coefficients of variation for 0.25 and 2.5 $\mu g \cdot ml^{-1}$ were 6 and 8% ($n = 10$) whereas the interassay coefficients of variation were 16 and 12% ($n = 28$), respectively.

In Vivo Protein Binding. Plasma protein binding was determined in vivo after administration of 2, 5, and 10 mg kg^{-1} in 5 min. For each dose level, three rats were used. From each rat, 2-ml blood samples were drawn at 5 and 25 min after administration of alphaxalone and collected in heparinized glass tubes. The tubes were centrifuged for 10 min at 5000 rpm to collect plasma. From each tube, two plasma samples of 50 μl were taken, and the remaining plasma was centrifuged at 37°C (15 min, 2000 relative centrifugal fields) using an ultrafiltrate device (Centrifree; Millipore, Bedford, MA). Two samples of at least 100 μl of ultrafiltrate were taken. After sample preparation, the plasma and ultrafiltrate samples were analyzed on the HPLC. The free fraction (f_u) was calculated by dividing

TABLE 1

Six treatment groups (A–F) with their corresponding administered amount of alphaxalone, infusion time, number of animals, vehicle, averaged body weight, and dose normalized for body weight (mean ± S.E.M.)

Vehicle was either 100 μl of DMSO or 100 μl of 25% (w/v) HPβCD.

Group	Amount	Infusion Time	*n*	Vehicle	Body Weight	Dose
	mg	*min*			*kg*	*mg · kg⁻¹*
A	0.50	5	8	DMSO	0.312 ± 0.011	1.62 ± 0.06
B	1.25	15	7	DMSO	0.342 ± 0.007[a]	3.67 ± 0.07
C	1.25	5	8	DMSO	0.263 ± 0.012[b]	4.83 ± 0.21
D	2.50	5	7	DMSO	0.349 ± 0.013[a]	7.21 ± 0.23
E	2.50	5	7	DMSO	0.264 ± 0.009	9.54 ± 0.84
F	2.50	5	7	HPβCD	0.280 ± 0.010	9.02 ± 0.96

[a] Significantly higher than E and F.
[b] Significantly lower than A, B, and D.

the free concentration in ultrafiltrate by the total (bound and free) concentration in plasma

Pharmacokinetic Data Analysis. In a population approach, the alphaxalone plasma concentration-time profiles of all individual rats in the different treatment groups were fitted simultaneously while explicitly taking into account both intraindividual variability in the model parameters as well as interindividual variability. A two-compartment model was selected for all compounds on the basis of the Akaike information criterion. The concentration-time courses were modeled according to the following equations.

$$\frac{dC_p}{dt} = \frac{\text{input} - Q \cdot C_p + Q \cdot C_t - \text{CL} \cdot C_p}{V_1} \quad (1)$$

$$\frac{dC_t}{dt} = \frac{Q \cdot C_p - Q \cdot C_t}{V_2} \quad (2)$$

in which C_p and C_t represent the concentration of alphaxalone in compartment 1 and 2, respectively. The input = R_0 for $t \leqq T$ and input = 0 for $t > T$, where R_0 and T are the zero-order infusion rate and the duration of infusion. In these equations CL is the clearance, Q is the intercompartmental clearance, V_1 and V_2 are the volumes of distribution of compartments 1 and 2.

The interindividual variability of these parameters was modeled according to an exponential equation.

$$P_i = \theta_i \cdot \exp(\eta_i) \quad (3)$$

where θ_i is the population estimate for parameter P, P_i is the individual estimate, and η_i is the random deviation of P_i from P. The values of η_i are assumed to be independently normally distributed with mean zero and variance ω^2. The residual error in the plasma drug concentration was characterized by a constant coefficient of variation error model.

$$Cm_{ij} = C_{p_{ij}} \cdot (1 + \varepsilon_{ij}) \quad (4)$$

where C_{pij} represents the jth plasma concentration for the ith individual predicted by the model. Cm_{ij} represents the prediction of concentration, and ϵ_{ij} accounts for the residual deviation of the model predicted value from the observed concentration. The value for ϵ was assumed to be independently normally distributed with mean zero and variance σ^2.

The model was implemented in the ADVAN6 subroutine in NONMEM (version V, NONMEM project group, University of California, San Francisco, CA). The first order estimation method with interaction (FOCE INTERACTION) was used to estimate the population θ, ω^2, and σ^2. From individual Bayesian post hoc parameter estimates, CL, Q, V_1, V_2, volume of distribution at steady state (V_{dss}) and two half-lives were calculated following standard procedures.

After covariate analysis and visual inspection, CL and Q were modeled as function of body weight.

$$\text{CL}_i = \theta_i \cdot \text{BW}_i^{\theta_j} \quad (5)$$

$$Q_i = \theta_i \cdot \text{BW}_i^{\theta_j} \quad (6)$$

where θj was assumed to be the same for CL and Q. V_1 and V_2 were estimated as a linear function of body weight.

$$V_1 = \theta_i \cdot \text{BW}_i \quad (7)$$

$$V_2 = \theta_i \cdot \text{BW}_i \quad (8)$$

Subsequently, the individual Bayesian post hoc pharmacokinetic parameter estimates were used to calculate the individual alphaxalone plasma concentrations at the time points of EEG measurements.

Hysteresis Minimization. Hysteresis was characterized on the basis of an effect-compartment model. In the effect-compartment approach, it is assumed that the rate of onset and offset of effect is governed by the rate of drug distribution to and from a hypothetical "effect-site" (Sheiner et al., 1979). Under this interpretation, the effect compartment is linked to the plasma compartment by a first order rate constant k_{1e} and with a rate constant for drug loss k_{eo}. The rate of change of the drug concentration in the effect compartment can then be expressed by the following differential equation.

$$\frac{dC_e}{dt} = k_{1e} \cdot C_p - k_{eo} \cdot C_e \quad (9)$$

where C_p represents the plasma concentration (see eq. 1 and 2) and C_e represents the effect-site concentration. Under the assumption that in equilibrium the effect-site concentration equals the plasma concentration, this equation can be simplified to

$$\frac{dC_e}{dt} = k_{eo} \cdot (C_p - C_e) \quad (10)$$

First, the equilibrium rate constant (k_{eo}) was calculated nonparametrically using the program keo-obj.exe (S. J. Shafer, Palo Alto Veterans Affairs Medical Center, Stanford University, Stanford, CA). Subsequently, hysteresis was minimized in a parametric approach. In the nonparametric approach, a concentration dependence was observed in k_{eo} parameter estimates. Therefore in the parametric model, k_{eo} was expressed as a function of the maximal observed concentration ($C_{\max}$).

$$k_{eo,app} = k_{eo} + \frac{k}{C_{\max} - C_{as}} \quad (11)$$

where $k_{eo,app}$ is the apparent in vivo k_{eo}, and k is a constant. For C_{as} the value of 1000 was chosen to position the asymptote, since all $C_{\max}$ levels that were reached were higher than 1000 ng $\cdot$ ml^{-1}. Replacing k_{eo} in eq. 10 by $k_{eo,app}$ we obtain

$$\frac{dC_e}{dt} = \left(k_{eo} + \frac{k}{C_{\max} - C_{as}} \right) \cdot (C_p - C_e) \quad (12)$$

The Mechanism-Based Model. In this investigation, amplitudes in the β-frequency range were used as measure of the drug response. The relationship between drug concentration and pharmacological effect is shown in Fig. 1. The drug, which is present at the effect-site, produces upon binding to the receptor a stimulus that is followed by a cascade of signal-transduction processes leading to the ultimate response. The definition of a drug-mediated response in terms of the occupation theory, first proposed by Stephenson and Furchgott (see Kenakin, 1997), consists of a drug receptor binding part resulting in a stimulus.

$$S = \frac{\in \cdot [R_t] \cdot C}{C + K_A} \quad (13)$$

where S is the stimulus as function of the concentration C. $\in$ represents the intrinsic efficacy of a drug to initiate a stimulus from one receptor, which is strictly a drug-related parameter, $[R_t]$ is the total number of receptors, K_A is the equilibrium dissociation constant of the drug from the receptor. This initial stimulus is then propagated into the observed pharmacological effect through a chain of postreceptor events, which is characterized by an unknown function f.

$$E = f(S) = f\left[\frac{\in \cdot [R_t] \cdot C}{C + K_A} \right] \quad (14)$$

Thus, drug-mediated responses in any given tissue depend on two tissue factors, $[R_t]$ and f, an unknown function, and two drug-related factors K_A and intrinsic efficacy $\in$. Two adjustments to this general model were made by Tuk and coworkers (1999) to apply the model to in vivo systems. First, the total amount of receptors cannot easily be measured in vivo, allowing only the product of $\in$ and $[R_t]$ to be estimated (Black and Leff, 1983). Second, the $\in [R_t]$ value of the drug

reaching the highest effect must be set to one, to allow an independent estimation of f and $\in [R_t]$. The relationship between effect-site drug concentration and effect is thus characterized by the following equation.

$$E = f(S) = f\left[\frac{e_{PD} \cdot C_e}{C_e + K_{PD}}\right] \quad (15)$$

where K_{PD} is the in vivo estimated affinity and e_{PD} is the in vivo estimated efficacy, relative to 1.

In a recent application of this model to characterize the relationship f between initial stimulus and observed pharmacological effects of benzodiazepines, a natural cubic spline was used, where the knots of the spline were placed at equidistant intervals on the stimulus axis (Tuk et al., 1999). Important characteristics of this relationship were the relatively small increase in effect at low stimulus intensities, the steeper increase in effect at higher stimulus intensities, and that no maximum was observed in this relationship. In this investigation, however, alphaxalone showed a biphasic EEG effect, and the maximal increase in effect was 2 to 3 times higher compared with benzodiazepines. Furthermore, at higher concentrations the effect decreased under baseline toward 0 μV (isoelectric EEG). This implied a physiological maximum of the stimulus (i.e., 0 μV is the maximal stimulus of 1). Therefore, the e_{PD} of alphaxalone was fixed at 1 in this receptor model (eq. 15). The relationship f between the initial stimulus (S) and the observed EEG effect (E) was characterized by a biphasic function.

$$E = E_{\text{top}} - a \cdot (S^d - b)^2 \quad (16)$$

which is a parabola if and only if d is equal to 1. In this equation, E_{top} represents the top of the parabola, a is a constant reflecting the slopes of the parabola, and $b^{1/d}$ is the stimulus for which the top of the parabola (i.e., the maximal effect) is reached. However, in the previous attempt to characterize the stimulus-effect relationship, Tuk et al. (1999) showed that the stimulus-effect relationship was defined by a small increase at low stimulus intensities and a steeper increase at higher stimulus intensities. This observation required that exponent d should be greater than 1 to result in a stimulus-effect relationship that has a shallow increase at low stimulus intensities and a steeper increase at higher stimulus intensities (see Fig. 1).

Rearranging eq. 16 results in

$$E = E_{\text{top}} - a \cdot (S^d)^2 + 2 \cdot a \cdot b \cdot S^d - a \cdot b^2 \quad (17)$$

When no drug is present the EEG is equal to its baseline value (E_0). Equations 16 and 17 then reduce to

$$E_0 = E_{\text{top}} - a \cdot b^2 \quad (18)$$

Substituting eq. 18 into eq. 17, and rearranging yields

$$E = E_0 - a \cdot ((S^d)^2 - 2 \cdot b \cdot S^d) \quad (19)$$

In this parametric model, individual plasma concentrations were fitted to the corresponding effects. The parameters $k_{eo,app}$, K_{PD}, a, and b were estimated and exponent d was fixed at 3. It was known that d should be greater than 1, and numerical evaluation revealed that the value of d was likely to be between 2 and 4. Averaged amplitudes over 40 min of individual EEG recordings before infusion served as input for individual baseline values. The interindividual variability in the pharmacodynamic parameters was modeled according to the exponential eq. 3. Similar to the pharmacokinetics, the residual variability in the pharmacodynamics was modeled as a constant coefficient of variation error according to eq. 4. To reduce the run-time, a two-step approach was applied in which first the individual estimates were obtained for the pharmacokinetic parameters. In the second step, the pharmacokinetic parameters were fixed at these values, and the pharmacodynamic parameters were obtained.

Statistical Analysis. Goodness-of-fit was analyzed on the basis of visual inspection and the value of the objective function. Model selection was based on the Akaike information criterion (Akaike, 1974) and assessment of parameter correlation. Statistical analysis was performed using one-way analysis of variance and a Tukey-Kramer multiple comparison test. In case of nonhomogeneity as determined by Bartlett's test, the nonparametric Kruskal-Wallis test was used. Statistical tests were performed using InStat version 3.0 for Windows (GraphPad Software, Inc., San Diego, CA). All data are represented as mean ± S.E.M and $p < 0.05$ was considered significant.

Results

Pharmacokinetics. Figure 2 shows the observed predicted population and individual alphaxalone plasma concentration time profiles for the six treatment groups. A two-compartment model best described the pharmacokinetic profiles, and pharmacokinetic parameters were found to be dependent on body weight. Population estimates and averaged Bayesian post hoc parameter estimates are summarized in Table 2. An exponential relationship between the values of the parameters CL and Q versus body weight was observed. CL and Q were defined as $158 \cdot \text{BW}^{1.67}$ and $143 \cdot \text{BW}^{1.67}$ (ml · min^{-1} · kg^{-1}), respectively. V_1 and V_2 were linearly dependent on body weight. For group A, post hoc parameter esti-

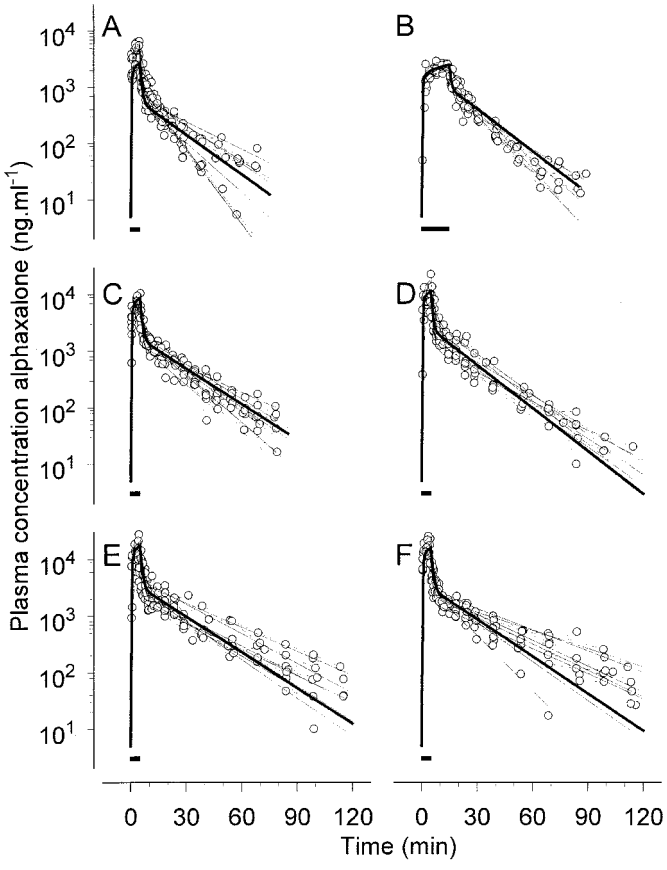

Fig. 2. Individual alphaxalone plasma concentration-time profiles for the treatment groups A-F. The observed concentrations (markers connected with dotted lines), the individual predictions (thin lines), and population predictions (thick lines) are depicted. The x-axis represents the time in minutes and the y-axis represents the plasma concentration of alphaxalone (ng · ml^{-1}) on a logarithmic scale. The black boxes represent the duration of the infusion.

mates for V_2 were significantly lower. However, for volume of distribution, a coefficient of variation of 48% was observed. Alphaxalone showed a distribution half-life of 0.8 ± 0.1 min and an elimination half-life of 14.2 ± 0.7 min (mean ± S.E.M., $n = 44$). The dose of 9 mg · kg^{-1} alphaxalone was administered in two vehicles (DMSO and HPβCD, groups E and F). Parameter estimates were not affected by the vehicle as is shown in Table 2. The free fraction of alphaxalone in plasma was 3.2 ± 0.3% ($n = 18$). Protein binding was independent of dose, concentration, or time.

In Vivo EEG Time Course of Alphaxalone. The observed and predicted EEG effect-time course and the predicted concentration time course of alphaxalone is depicted in Fig. 3 for representative individuals in each treatment group. The EEG effects, expressed as absolute amplitude in 11.5 to 30 Hz band versus time, revealed a biphasic pattern. Upon the start of the infusion, the amplitude immediately increased, followed by a partial decrease. After the end of the infusion, effect returned to the same height and then gradually returned to baseline. The partial decrease in amplitude appeared to be correlated to a state of unconsciousness of the rats and was deeper with higher dosages. Baseline EEG effect was 10.6 ± 0.3 μV (mean ± S.E.M., $n = 44$) and similar for each group. Visual inspection revealed that the initial and second peak reached equal heights in each individual rat and were defined as E_{top} in the model. The depth of the partial decrease increased with dose and reached amplitudes of only 0 to 3 μV (isoelectric EEG) with the highest dosages (E and F). The first EEG peak was reached within 0 to 2 min during infusion except for the 15-min infusion, where the first peak was reached after ~5 min. The second peak was reached between 5 and 25 min after stopping the infusion and was later with higher dosages.

The maximal increase in EEG effect upon baseline of alphaxalone (22 μV) was 2 to 3 times higher compared with the monophasic patterns of benzodiazepines, such as for diazepam, which revealed a maximum increase of 9 μV in the same experimental set-up (unpublished observations). Also in contrast to benzodiazepines, alphaxalone showed a biphasic effect-time course in all frequency bands. In control experiments, the vehicles DMSO and HPβCD did not affect the EEG amplitudes (data not shown).

Hysteresis. All individual plasma concentration-effect relationships were biphasic and showed a hysteresis loop (see Fig. 4, left panel). The maximal increase in effect was the same for each individual and dose. At ~250 ng · ml^{-1} the amplitudes started to increase and E_{top} was reached at a concentration of ~1000 ng · ml^{-1}. Midpoint location for the increasing limb of the concentration-effect relationship was ~550 ng · ml^{-1}. The decreasing limb, at concentrations higher than ~1000 ng · ml^{-1} showed a larger hysteresis loop at higher concentrations, as shown in Fig. 4, left panel.

Hysteresis was minimized both nonparametrically (k_{eo}-nonpar) and parametrically (k_{eo}-par). With both methods, the hysteresis loop could be successfully minimized, although the parametric approach yielded more accurate parameter estimates. Estimates of k_{eo} were lower with increasing concentrations (reflecting the increase in loop with higher dosages) as depicted in Table 3 and in Fig. 5. Estimation of k_{eo} as a function of the maximal reached concentration ($k_{eo,app}$) successfully minimized the concentration-dependent hysteresis. Maximal hysteresis with the highest dosages showed that the k_{eo} for alphaxalone is 0.33 ± 0.08 min^{-1}, which corresponds to a half-life of k_{eo} of 2.1 min. Estimates for $k_{eo,app}$ were not different from k_{eo}-nonpar and k_{eo}-par, except for group C. Although the plasma kinetics and time course of pharmacological effect varied, the apparent effect-site concentration-effect relationship was consistent between animals (see Fig. 4, right panel).

Mechanism-Based PK/PD Modeling. In the mechanism-based PK/PD approach, the plasma concentrations and EEG effects were fitted using the mechanism-based model and the link model. All the individual plasma concentration-effect profiles were successfully described using the mechanism-based PK/PD model, yielding estimates for $k_{eo,app}$, K_{PD}, a and b. The pharmacodynamic parameter estimates are depicted in Table 4. Figure 3 shows the predicted effect versus time profile, and Fig. 4 shows the predicted plasma concentration and predicted effect-site concentration versus effect relationship for representative rats. The relationship for the effect-site concentration versus stimulus for all rats ($n = 44$) is shown in Fig. 6A. Population K_{PD} was estimated at 432 ± 26 ng · ml^{-1}, whereas e_{PD} was fixed at 1, due to the fact that the effects at maximal stimulus reached a physiological maximum. The mean parameter estimates for K_{PD} did not significantly differ between the groups, although groups A and F were slightly outside the 95% confidence interval of the population estimate. In Fig. 6B, the biphasic stimulus-effect relationship for all individual rats ($n = 44$) is shown. The stimulus-effect relationship was described using eq. 16:

TABLE 2

Population pharmacokinetic parameter estimates for CL, Q, V_1, and V_2 with corresponding interindividual coefficient of variation (CV) and 95% confidence interval (CI)

Below the population estimates, the averaged individual Bayesian post hoc pharmacokinetic parameter estimates are given for treatment groups A through F (mean ± S.E.M.). The intraindividual residual error was 26.5%.

	n	CL	Q	V_1	V_2
		$ml \cdot min^{-1} \cdot kg^{-1}$		$ml \cdot kg^{-1}$	
Population		158 ± 29	143 ± 31	122 ± 20	606 ± 48
CV		27%	47%	49%	48%
95% CI		98 –216	80 –206	82 –162	510 –701
Group					
A	8	124 ± 12	101 ± 19	108 ± 18	364 ± 46[a]
B	7	175 ± 8	169 ± 12	173 ± 10	605 ± 63
C	8	181 ± 10	185 ± 16	131 ± 13	674 ± 62
D	7	171 ± 16	167 ± 26	160 ± 26	804 ± 131
E	7	168 ± 17	169 ± 19	99 ± 6	787 ± 84
F	7	154 ± 15	135 ± 13	98 ± 7	775 ± 66

[a] Significantly lower than groups D, E, and F ($p < 0.05$).

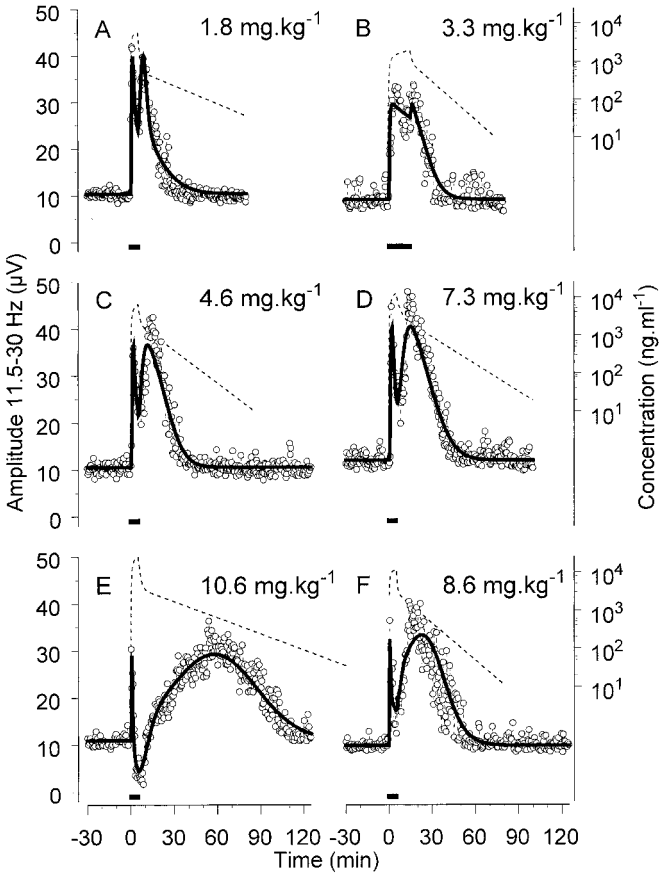

Fig. 3. Changes in amplitude in the β frequency range in time following administration of alphaxalone. For each treatment group (A–F) a representative observed (dots) and predicted (thick line) effect-time profile is shown. The black boxes represent infusion duration. Time (min) is given on the x-axis and the amplitude in the b frequency range (μV) is given on the left y-axis. The corresponding plasma concentration (ng · ml^{-1}, dotted line) in time is depicted on the right y-axis on a logarithmic scale. The individual dose is depicted in the graph.

$E = 32 \pm 0.8 - 108 \pm 6 \cdot (S^3 - 0.44 \pm 0.01)^2$. Calculating E_{top} from individual E_0 using eq. 18 and averaging resulted in the value for E_{top}: 32.0 $\pm$ 0.8 μV (mean $\pm$ S.E.M., n = 44). Mean post hoc parameter estimates for a and b were not significantly different between the groups. The intraindividual residual variability was 16%. The drug-receptor interaction and the following stimulus-effect relationship were consistent for all animals and treatment groups.

Discussion

Alphaxalone Pharmacokinetics. Alphaxalone pharmacokinetics were successfully described by a two-compartment model. The observed alphaxalone distribution and elimination half-life (0.8 and 14 min, respectively) are in agreement with a previous investigation, reporting a half-life of 7 min (Child et al., 1972). The clearance of alphaxalone (158 · BW$^{1.67}$ ml · min^{-1} · kg^{-1}) was approximately equal to the rat liver blood flow (~20 ml · min for a rat weighing 300 g). Blood flow-dependent elimination can explain that body weight was an important covariate of the clearance. It has been shown that alphaxalone is rapidly metabolized to inactive metabolites by the hepatic mixed function oxygenase system (Sear and McGivan, 1981). A fast hepatic clearance and low oral bioavailability was also reported for humans (Sear, 1996). The volume of distribution (V_2) for the lowest dose (group A) was significantly lower than for the other groups. An explanation might be that the mean protein-binding is different in this group or alternatively, that there is a dose-dependent (fat) tissue distribution. It has been reported that alphaxalone exhibits a uniform distribution throughout the body, except for a slight accumulation in the fat and brain tissue (Pastorino et al., 1979). A Michaelis-Menten type of pharmacokinetic elimination was unlikely, since in this investigation the maximum in vivo concentrations (C_{max}) of alphaxalone only exceeded the in vitro K_m for cytochrome P450 (~8.3 μg/ml; Sear and McGivan, 1981) at dosages higher than 9 mg · kg^{-1}.

In this investigation, the plasma protein-binding of alphaxalone was ~97% and no dose, concentration, or time dependence was observed. Child et al. (1972) reported a protein-binding between 35 and 44% in rats. However, it cannot be excluded in that study that unbound metabolites of alphaxalone were a masking factor, since protein-binding was measured using radioactive-labeled alphaxalone in contrast to our sensitive and selective HPLC method. A qualitative determination showed that alphaxalone binds to albumin and β-lipoprotein in rats (Jones, 1972).

Hydroxypropyl-β-cyclodextrin did not alter alphaxalone pharmacokinetic and pharmacodynamic parameter esti-

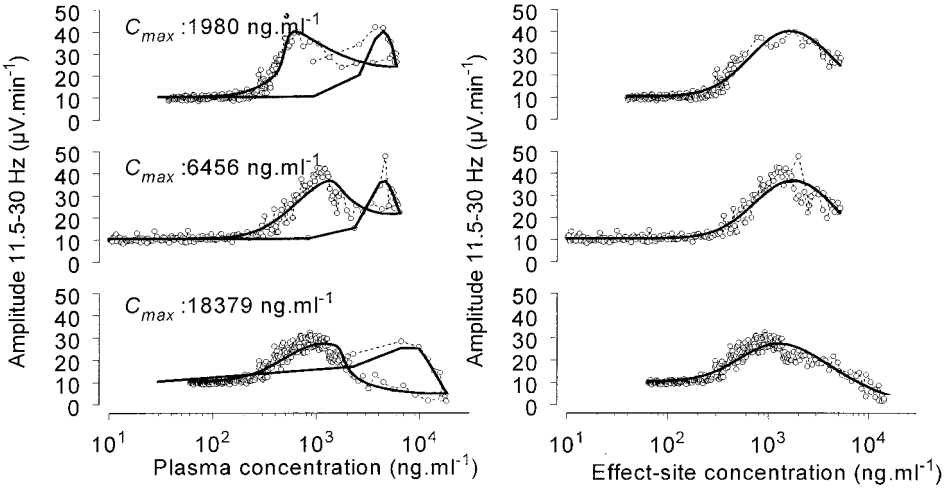

Fig. 4. Left panel, observed and predicted alphaxalone plasma concentration versus EEG effect in the b frequency range for three representative rats that differ in maximal plasma concentrations (C_{max}). The value for C_{max} is depicted in the graphs. In each graph the increasing effect at low concentrations (<1000 ng · ml^{-1}) shows a similar profile independent of dose, whereas at high concentrations (>1000 ng · ml^{-1}) the hysteresis loop increases with increasing maximal concentrations. Right panel, observed and predicted alphaxalone effect-site concentration versus EEG amplitude in the β frequency range after minimizing hysteresis.

TABLE 3

Mean parameter estimates of k_{eo} for groups A through F

The value of k_{eo} was estimated nonparametrically (k_{eo}-nonpar), parametrically (k_{eo}-par), and parametrically ($k_{eo,app}$) with maximal plasma concentrations (C_{max}) as covariate. The concentration-dependent hysteresis was defined as

$$k_{eo,app} = 0.325 \pm 0.08 + \frac{1150}{C_{max} - 1000}(min^{-1}).$$

Group	n	k_{eo}-nonpar	k_{eo}-par	C_{max}	$k_{eo,app}$
		min^{-1}	min^{-1}	$ng \cdot ml^{-1}$	min^{-1}
A	8	1.34 ± 0.30	1.20 ± 0.31	4075 ± 481	0.82 ± 0.09
B	7	1.78 ± 0.43	1.73 ± 0.40	1735 ± 112	2.09 ± 0.23
C	8	0.35 ± 0.04	0.31 ± 0.03	7699 ± 542	0.47 ± 0.01[a]
D	7	0.35 ± 0.08	0.35 ± 0.06	10678 ± 1452	0.41 ± 0.03
E	7	0.33 ± 0.04	0.42 ± 0.07	16246 ± 1993	0.39 ± 0.02
F	7	0.47 ± 0.05	0.43 ± 0.06	17095 ± 1752	0.45 ± 0.04

[a] Significantly higher than for k_{eo}-par and k_{eo}-nonpar ($p < 0.05$).

mates (groups E versus F). This was also reported for the bioavailability and onset of effect of pregnanolone and pregnenolone (Brewster et al., 1995).

Alphaxalone Pharmacodynamics and Hysteresis. The biphasic pattern and counter clockwise hysteresis, observed for the concentration-effect relationship of alphaxalone, are common for general anesthetics (Mandema and Danhof, 1990; Ebling et al., 1991; Mandema et al., 1991; Cox et al., 1998b). In all these reports hysteresis has been minimized by postulating a hypothetical effect-compartment. For propofol and thiopental, the values for the half-life k_{eo} were between 1 and 3 min (Ebling et al., 1991; Cox et al., 1998b), which is the same range as alphaxalone. In these investigations, the resolution of concentration-effect data was not always sufficient to be able to detect concentration-dependent hysteresis. Some indication for similar concentration dependence of k_{eo} might be that Mandema and Danhof (1990) have reported that two equilibration rate constants existed for dual effects of heptabarbital. And in another report nonsteady-state conditions for equilibration rate constants have been assessed by the estimation of a biophase equilibrium time (Mandema et al., 1991).

An explanation for the concentration dependence of k_{eo} may be the occurrence of concentration-dependent cardiovascular or hemodynamic side-effects. Administration of alphaxalone has been shown to affect heart-rate and aortic pressure in the rat and man in a concentration-dependent manner (Sear, 1996). Other i.v. anesthetic agents such as thiopental and propofol in most conditions also cause a drop in cerebral blood flow and consequently diminish their own rate of transport to the brain assuming that this transport is perfusion rate-limited (Upton et al., 2000). Another explanation for the concentration-dependent hysteresis might be a saturable transport to the site of action, to the brain. However, to date, no specific neuroactive steroid transporters have been demonstrated at the blood-brain barrier. Calculation of polar surface area indicated that alphaxalone should be able to pass the blood-brain barrier easily by the transcellular route (Kelder et al., 1999).

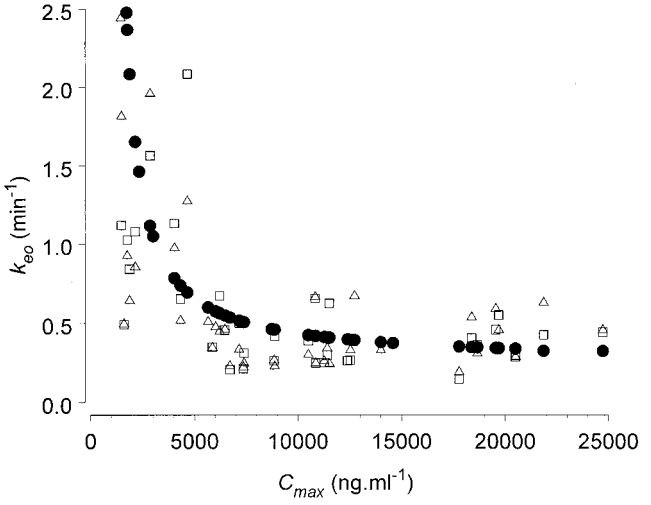

Fig. 5. Nonparametric (squares) and parametric (triangles) k_{eo} estimates and $k_{eo,app}$ as a function of C_{max} (filled circles): $k_{eo,app} = 0.325 \pm 0.08 + ((1150/(C_{max} - 1000))$. The maximal plasma concentration measured for each individual (C_{max}) is depicted on the x-axis and values for k_{eo} and $k_{eo,app}$ on the y-axis.

Mechanism-Based PK/PD Modeling. Although several methods have been described to characterize biphasic drug concentration-effect relationships, all these approaches are rather empirical (Mandema and Danhof, 1990; Ebling et al., 1991; Dutta and Ebling, 1997). In the present investigation we have developed a mechanism-based PK/PD approach to describe the biphasic concentration-effect relationship of alphaxalone. Although the parabolic stimulus-response function is an empirical equation, the separation of the drug-receptor interaction from the biphasic stimulus-response relationship is an important feature of this mechanism-based PK/PD model. In principle the drug-specific properties (i.e., receptor affinity and intrinsic efficacy) can be determined in

TABLE 4

Population pharmacodynamic parameter estimates (groups A–F) for K_{PD}, a, and b with corresponding coefficient of variation (CV) and 95% confidence interval (CI)

E_0 was 10.6 ± 0.3 μV and E_{top} was 32 ± 0.8 μV (mean ± S.E.M., n = 44). Exponent d was fixed at 3. Below the population estimates, the averaged individual Bayesian post hoc pharmacokinetic parameter estimates are given for treatment groups A through F (mean ± S.E.M.). Intraindividual residual variation was 16%.

	n	K_{PD}	a	b
		$ml \cdot min^{-1}$		
Population		432 ± 26	108 ± 6	0.44 ± 0.01
CV		31%	23%	7%
95% CI		380–484	95–121	0.42–0.46
Group				
A	8	491 ± 34	117 ± 6	0.44 ± 0.01
B	7	438 ± 26	113 ± 9	0.41 ± 0.01
C	8	437 ± 34	119 ± 6	0.45 ± 0.01
D	7	482 ± 30	108 ± 9	0.44 ± 0.01
E	7	412 ± 60	102 ± 9	0.45 ± 0.01
F	7	375 ± 28	97 ± 5	0.46 ± 0.01

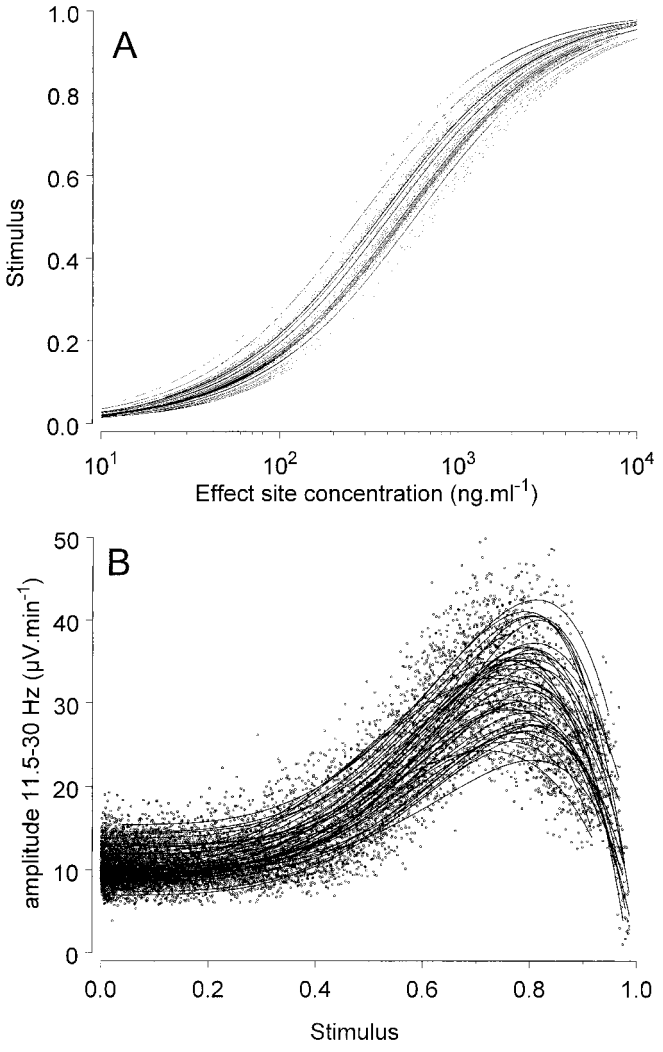

Figure 6. Panel A, drug-receptor interaction. The relationship between effect-site concentration and stimulus for alphaxalone for all individuals (n = 44). Effect-site concentration (ng · ml^{-1}) is depicted on the x-axis, and the stimulus is depicted on the y-axis. Panel B, stimulus-effect relationship. The predicted biphasic stimulus-effect relationship for all individuals (n = 44) is shown. Dots represent the observed amplitudes, and the thin lines represent the best-fitted individual lines by the parabolic stimulus-effect model. Intraindividual variability is 16%.

in vitro test systems. The system-related properties (related to transduction processes) on the other hand can only be obtained in vivo. The latter are unique in the sense that they are identical regardless of the drug that is administered.

An important example of a mechanism-based model is the operational model of agonism (Black and Leff, 1983). This model is based on the assumption that the unique stimulus-effect relationship is hyperbolic in nature. Recently, this model has been successfully applied in in vivo investigations to predict tissue selectivity for low efficacy adenosine A_1 receptor agonists (Van der Graaf et al., 1999), receptor reserve for μ-opioid receptor agonists (Cox et al., 1998a) and to explain functional adaptation in epilepsy models (Cleton et al., 1999b). In another mechanism-based modeling approach, based on the occupancy receptor theory, a stimulus-effect relationship was found for benzodiazepines, which was a nonparameterized monotonously increasing function without a maximum (Tuk et al., 1999).

In the present investigation, alphaxalone revealed a 2 to 3 times higher increase in absolute EEG effect relative to benzodiazepines, which indicated a system maximum of the EEG. Furthermore, a decrease in amplitudes at high concentrations was observed which decreased under baseline and reached isoelectric EEG (i.e., physiological minimum). Based on literature, a biphasic stimulus-EEG effect relationship upon binding was proposed, which should be unique for this system. In this investigation, this biphasic stimulus-response relationship was characterized, whereas in subsequent investigations, the mechanism-based PK/PD model is validated. Other neuroactive steroids, like alphaxalone, show all biphasic concentration-response relationships in vivo (unpublished observations).

It is known that neuroactive steroids are general anesthetics, which act by selective binding on ligand-gated ion channels, specifically at the $GABA_A$ receptor (Yamakura et al., 2001). Neuroactive steroids, but also barbiturates, show biphasic EEG effects in vivo. Although much has been reported about the cause of biphasic effects, still no definite consensus has been reached. One explanation, which can be ruled out, is the formation of a metabolite that acts as an antagonist on the EEG effect at higher concentrations. It has been shown that alphaxalone is rapidly metabolized only into metabolites that are pharmacologically inactive (Child et al., 1972; Sear and McGivan, 1981).

An explanation that suggests the involvement of several receptor systems with opposite effects (Paalzow and Edlund, 1979) is unlikely. Although brain region-dependent variation in binding and function of $GABA_A$ receptor has been reported (Lambert et al., 1995; Yamakura et al., 2001), it appears that the biphasic effects of neuroactive steroids are not related to receptor heterogeneity but that in various tissues the efficacy of $GABA_A$ receptor modulators varies due to the dual actions that they have on $GABA_A$ receptor channels: i.e., the allosteric modulation of GABA binding and direct channel activation at higher concentrations (Srinivasan et al., 1999). It has been shown that neuroactive steroids can produce biphasic responses via single neurons (MacIver and Roth, 1987; Dallwig et al., 1999), (recombinant) receptors (Lambert et al., 1995; Hill Venning et al., 1996), and in hippocampal CA1 pyramidal cell (Burg et al., 1998). This is in agreement with another report that suggested that $GABA_A$ receptor response may change from inhibitory to excitatory, depending on the frequency (i.e., intensity) of stimulation (Archer and Roth, 1999). The fact that other $GABA_A$ receptor ligands such as barbiturates showed biphasic EEG effects supports the suggestion that the transduction cascade leading to the effect which follows the receptor activation is biphasic.

The estimated in vivo K_{PD} for alphaxalone of 432 ± 26 ng · ml^{-1} is in the range of values reported for the (indirect) inhibition of ^{35}S-t-butylbicyclophosphorothionate binding by alphaxalone, for which the IC_{50} varied between 110 and 180 ng · ml^{-1} (Hill Venning et al., 1996; Anderson et al., 1997) and values reported for in vitro functional studies with recombinant receptors, for which the EC_{50} was ~730 ng · ml^{-1} (Hill Venning et al., 1996). Using this mechanism-based PK/PD approach for the determination of the in vivo K_{PD} will allow comparison between biphasic EEG effects of other compounds, but also between these biphasic EEG effects and other pharmacodynamic endpoints in vivo and in vitro studies.

In conclusion, in this mechanism-based PK/PD approach, in vivo biphasic concentration-effect relationships have been successfully described. The in vivo affinity of alphaxalone was estimated and a biphasic stimulus-effect relationship was parameterized. This mechanism-based biphasic PK/PD model can be further extended in the investigation of $GABA_A$ receptor modulation by other neuroactive steroids and benzodiazepines.

Acknowledgments

We gratefully acknowledge Erica Tukker for excellent technical assistance.

References

Akaike H (1974) A new look at the statistical model identification. *IEEE Trans Automat Control* **AC-19:**716–723.

Anderson A, Boyd AC, Byford A, Campbell AC, Gemmell DK, Hamilton NM, Hill DR, Hill Venning C, Lambert JJ, Maidment M, et al. (1997) Anesthetic activity of novel water soluble 2 beta morpholinyl steroids and their modulatory effects at GABA(A) receptors. *J Med Chem* **40:**1668–1681.

Archer DP and Roth SH (1999) Acetazolamide and amiloride inhibit pentobarbital-induced facilitation of nocifensive reflexes. *Anesthesiology* **90:**1158–1164.

Black JW and Leff P (1983) Operational models of pharmacological agonism. *Proc R Soc Lond B* **220:**141–162.

Brewster ME, Anderson WR, Loftsson T, Huang MJ, Bodor N, and Pop E (1995) Preparation, characterization and anesthetic properties of 2- hydroxypropyl-beta-cyclodextrin complexes of pregnanolone and pregnenolone in rat and mouse. *J Pharm Sci* **84:**1154–1159.

Burg M, Heinemann U, and Schmitz D (1998) Neuroactive steroids induce GABAA receptor-mediated depolarizing postsynaptic potentials in hippocampal ca1 pyramidal cells of the rat. *Eur J Neurosci* **10:**2880–2886.

Child KJ, Gibson W, Harnby G, and Hart JW (1972) Metabolism and excretion of Althesin (CT 1341) in the rat. *Postgrad Med J* **48 (Suppl 2):**37–43.

Cleton A, De Greef HJ, Edelbroek PM, Voskuyl RA, and Danhof M (1999a) Application of a combined "effect compartment/indirect response model" to the central nervous system effects of tiagabine in the rat. *J Pharmacokinet Biopharm* **27:**301–323.

Cleton A, Van der Graaf PH, Ghijsen W, Voskuyl R, and Danhof M (1999b) Mechanism-based modeling of adaptive changes in the pharmacodynamics of midazolam in the kindling model of epilepsy. *Pharm Res* **16:**1702–1709.

Cottrell GA, Lambert JJ, and Peters JA (1987) Modulation of GABAA receptor activity by alphaxalone. *Br J Pharmacol* **90:**491–500.

Cox EH, Kerbusch T, Van der Graaf PH, and Danhof M (1998a) Pharmacokinetic-pharmacodynamic modeling of the electroencephalogram effect of synthetic opioids in the rat: correlation with the interaction at the mu-opioid receptor. *J Pharmacol Exp Ther* **284:**1095–1103.

Cox EH, Knibbe CA, Koster VS, Langemeijer MW, Tukker EE, Lange R, Kuks PF, Langemeijer HJ, Lie AHL, and Danhof M (1998b) Influence of different fat emulsion-based intravenous formulations on the pharmacokinetics and pharmacodynamics of propofol. *Pharm Res* (*NY*) **15:**442–448.

Dallwig R, Deitmer JW, and Backus KH (1999) On the mechanism of GABA-induced currents in cultured rat cortical neurons. *Pfluegers Arch* **437:**289–297.

Danhof M and Mandema JW (1992) Modeling of the pharmacodynamics and pharmacodynamic interactions of CNS active drugs. *Int J Clin Pharmacol Ther Toxicol* **30:**516–519.

Dutta S and Ebling WF (1997) Parameter estimability of biphasic response models. *J Pharm Sci* **86:**44–51.

Ebling WF, Danhof M, and Stanski DR (1991) Pharmacodynamic characterization of the electroencephalographic effects of thiopental in rats. *J Pharmacokinet Biopharm* **19:**123–143.

Gasior M, Carter RB, and Witkin JM (1999) Neuroactive steroids: potential therapeutic use in neurological and psychiatric disorders. *Trends Pharmacol Sci* **20:** 107–112.

Hill Venning C, Peters JA, Callachan H, Lambert JJ, Gemmell DK, Anderson A, Byford A, Hamilton N, Hill DR, Marshall RJ, and Campbell AC (1996) The anaesthetic action and modulation of GABAA receptor activity by the novel water-soluble aminosteroid Org 20599. *Neuropharmacology* **35:**1209–1222.

Jones BC (1972) The protein binding of alphaxalone. *Postgrad Med J* **48 (Suppl 2):**47–51.

Kelder J, Grootenhuis PD, Bayada DM, Delbressine LP, and Ploemen JP (1999) Polar molecular surface as a dominating determinant for oral absorption and brain penetration of drugs. *Pharm Res* (*NY*) **16:**1514–1519.

Kenakin T (1997) Drug receptor theory, in *Pharmacological Analysis of Drug-Receptor Interaction*, pp 1–42, Lippincott-Raven Publishers, Philadelphia, PA.

Lambert JJ, Belelli D, Hill Venning C, and Peters JA (1995) Neurosteroids and GABAA receptor function. *Trends Pharmacol Sci* **16:**295–303.

MacIver MB and Roth SH (1987) Anesthetics produce differential actions on the discharge activity of a single neuron. *Eur J Pharmacol* **139:**43–52.

Mandema JW and Danhof M (1990) Pharmacokinetic-pharmacodynamic modeling of the central nervous system effects of heptabarbital using aperiodic EEG analysis. *J Pharmacokinet Biopharm* **18:**459–481.

Mandema JW, Veng PP, and Danhof M (1991) Estimation of amobarbital plasma-effect site equilibration kinetics. Relevance of polyexponential conductance functions. *J Pharmacokinet Biopharm* **19:**617–634.

Paalzow LK and Edlund PO (1979) Multiple receptor responses: a new concept to describe the relationship between pharmacological effects and pharmacokinetics of a drug: studies on clonidine in the rat and cat. *J Pharmacokinet Biopharm* **7:**495–510.

Pastorino AM, Favaretto P, and Vallaperta P (1979) Alphaxalone distribution in rat tissues. *Arzneim-Forsch* **29:**204–206.

Paul SM and Purdy RH (1992) Neuroactive steroids. *FASEB J.* **6:**2311–2322.

Sear JW (1996) Steroid anesthetics: old compounds, new drugs. *J Clin Anesth* **8:**91S–98S.

Sear JW and McGivan JD (1981) Metabolism of alphaxalone in the rat: evidence for the limitation of the anaesthetic effect by the rate of degradation through the hepatic mixed function oxygenase system. *Br J Anaesth* **53:**417–424.

Seyle H (1942) Correlations between the chemical structure and the pharmacological actions of the steroids. *Endocrinology* **30:**437–453.

Sheiner LB, Stanski DR, Vozeh S, Miller RD, and Ham J (1979) Simultaneous modeling of pharmacokinetics and pharmacodynamics: application to d-tubocurarine. *Clin Pharmacol Ther* **25:**358–371.

Srinivasan S, Sapp DW, Tobin AJ, and Olsen RW (1999) Biphasic modulation of GABA(A) receptor binding by steroids suggests functional correlates. *Neurochem Res* **24:**1363–1372.

Tuk B, van Oostenbruggen MF, Herben VM, Mandema JW, and Danhof M (1999) Characterization of the pharmacodynamic interaction between parent drug and active metabolite in vivo: midazolam and alpha-OH-midazolam. *J Pharmacol Exp Ther* **289:**1067–1074.

Upton RN, Ludbrook GL, Grant C, and Doolette DJ (2000) The effect of altered cerebral blood flow on the cerebral kinetics of thiopental and propofol in sheep. *Anesthesiology* **93:**1085–1094.

Van der Graaf PH and Danhof M (1997) Analysis of drug-receptor interactions in vivo: a new approach in pharmacokinetic-pharmacodynamic modelling. *Int J Clin Pharmacol Ther* **35:**442–446.

Van der Graaf PH, Van Schaick EA, Visser SAG, De Greef HJ, IJzerman AP, and Danhof M (1999) Mechanism-based pharmacokinetic-pharmacodynamic modeling of antilipolytic effects of adenosine A(1) receptor agonists in rats: prediction of tissue-dependent efficacy in vivo. *J Pharmacol Exp Ther* **290:**702–709.

Verotta D and Sheiner LB (1987) Simultaneous modeling of pharmacokinetics and pharmacodynamics: an improved algorithm. *Comput Appl Biosci* **3:**345–349.

Visser SAG, Smulders CJGM, Gladdines WWFT, Irth H, Van der Graaf PH, and Danhof M (2000) High-performance liquid chromatography of the neuroactive steroids alphaxalone and pregnanolone in plasma using dansyl hydrazine as fluorescent label: application to a pharmacokinetic-pharmacodynamic study in rats. *J Chromatogr B Biomed Sci Appl* **745:**357–363.

Yamakura T, Bertaccini E, Trudell JR, and Harris RA (2001) Anesthetics and ion channels: molecular models and sites of action. *Annu Rev Pharmacol Toxicol* **41:**23–51.

Zuideveld KP, Maas HJ, Treijtel N, Hulshof J, Der Graaf PH, Peletier LA, and Danhof M (2001) A set-point model with oscillatory behavior predicts the time course of 8-OH-DPAT-induced hypothermia. *Am J Physiol Regul Integr Comp Physiol* **281:**R2059–R2071.

Address correspondence to: Prof. Dr. Meinert Danhof, Division of Pharmacology, Leiden/Amsterdam Center for Drug Research, Leiden University, P.O. Box 9503, 2300 RA Leiden, The Netherlands. E-mail: m.danhof@ LACDR. LeidenUniv.nl .0.0.0.0